Available online at www.sciencedirect.com
ScienceDirect
Trans. Nonferrous Met. Soc. China 25(2015) 3974−3979
Transactions of Nonferrous Metals Society of China
www.tnmsc.cn

Preparation and photoelectric properties of Ho^{3+}-doped titanium dioxide nanowire downconversion photoanode

Yue-ying LI[1,2,3], Hong-shun HAO[1,2,3], Li-jun WANG[1,2,3], Wei-hua GUO[1,2,3], Qing SU[1,2,3], Lei QIN[3], Wen-yuan GAO[1,2,3], Gui-shan LIU[1,2,3], Zhi-qiang HU[1,2,3]

1. Department of Inorganic Nonmetallic Materials Engineering, Dalian Polytechnic University, Dalian 116034, China;
2. Liaoning Provincial College Key Laboratory of New Materials and Material Modification, Dalian Polytechnic University, Dalian 116034, China;
3. National Engineering Research Center of Seafood, Dalian Polytechnic University, Dalian 116034, China

Received 22 December 2014; accepted 17 June 2015

Abstract: Ho^{3+}-doped titanium dioxide (TiO_2:Ho^{3+}) downconversion (DC) nanowires were synthesized through a simple hydrothermal method followed by a subsequent calcination process after being immersed in $Ho(NO_3)_3$ aqueous solution. Moreover, TiO_2:Ho^{3+} nanowires (HTNWs) were used as the photoanode in dye-sensitized solar cells (DSSCs) to investigate their photoelectric properties. Scanning electron microscopy (SEM) and X-ray diffraction (XRD) were used to characterize the morphology and structure of the material, respectively. The photofluorescence and ultraviolet−visible absorption spectra of HTNWs reveal a DC from the near and middle ultraviolet light to visible light which matches the strong absorbed region of the N719 dye. Compared with the pure TNW photoanode, HTNWs DC photoanodes show greater photovoltaic efficiency. The photovoltaic conversion efficiency (η) of the DSSCs with HTNWs photoanode doped with 4% Ho_2O_3 (mass fraction) is two times that with pure TNW photoanode. This enhancement could be attributed to HTNWs which could extend the spectral response range of DSSCs to the near and middle ultraviolet region and increase the short-circuit current density (J_{sc}) of DSSCs, thus leading to the enhancement of photovoltaic conversion efficiency.

Key words: Ho^{3+}-doped titanium dioxide nanowire; downconversion fluorescence; dye-sensitized solar cells; photovoltaic performance

1 Introduction

Because of its low cost and simple fabrication method, clean renewable energy utilization has become one of the primary underlying solutions for global warming [1], and improving the dye-sensitized solar cells (DSSC) efficiency has been of great significance for many research groups. To date, many investigators have pursed novel methods to enhance the battery performance based on the development of better elements, such as sensitizing dyes [2,3], transparent conducting oxides (TCOs) [4], redox electrolytes [5], nanocrystalline TiO_2 layers [6,7], and Pt counter electrodes [8]. Particularly, on account of the direct influence of nanocrystalline TiO_2 layer on the light harvesting, charge recombination and interfacial contact of the electrodes/electrolytes, it is a vital component in DSSCs. Nevertheless, the electrons generated by disordered TiO_2 films may suffer a series of trapping events between trap states on neighboring particles or recombine with oxidizing species in the electrolyte during random walking through the film, leading to the limitation of the charge-collection efficiency [9,10]. Hence, many attempts have been made to study TiO_2 nanofibers or nanowires for their promising microstructure and satisfied photoelectric property in energy utilization [11,12].

In addition, DSSCs have the maximum absorption up to 800 nm of the total incident solar irradiation [13]. This brings out a major issue for this technology because the unutilized ultraviolet and infrared occupy 50% of solar irradiation, and limits the solar energy conversion efficiency for DSSCs. Therefore, extending the spectral

Foundation item: Project (2012FU125X03) supported by Open Research Fund Project of National Engineering Research Center of Seafood, China; Project (2011–191) supported by the Key Science and Technology Platform of Liaoning Provincial Education Department, China; Project (2010–354) supported by the Science and Technology Platform of Dalian, China
Corresponding author: Hong-shun HAO; Tel: +86-411-86323708; E-mail: beike1952@163.com
DOI: 10.1016/S1003-6326(15)64046-8

response range of DSSCs to the ultraviolet region has become a vital approach to increase the DSSCs efficiency. Many researchers used rare earth metal ions as the catalysts for their incompletely occupied 4f and empty 5d orbits [14]. Doped rare-earth compound can not only increase the photocurrent via conversion luminescence, but also improve the photovoltage by p-type doping effect. So far, rare-earth doped TiO_2 has been widely studied [15,16]. Compared with pure TiO_2-DSSC, all other lanthanide metal ions such as Nd, Eu, Gd and Sm doped TiO_2-DSSCs show an improvement in the performance of DSSCs [17,18]. In the previous work [19], $SrTiO_3$:Ho^{3+} nanoparticles were prepared and it was proved that the introduction of Ho^{3+} could increase the efficiency by 59%. But to our best knowledge, the investigation on the application of TiO_2:Ho^{3+} nanowire on DSSCs has rarely been reported.

In the present study, TiO_2:Ho^{3+} nanowires (HTNWs) were prepared through hydrothermal process in alkali liquid-based system followed by a subsequent calcination process after being immersed in $Ho(NO_3)_3$ aqueous solutions overnight. The Ho^{3+}-doped content that crucially affects the microstructure and optical properties of the synthesized nanowires was optimized. Then, the morphology and crystal structure of the samples were studied. Finally, the effect of produced nanowires on the performance of DSSCs was investigated.

2 Experimental

2.1 Synthesis of HTNWs

2.1.1 Synthesis of HTNWs precursor

Appropriate TiO_2 (Degussa P25) was added to NaOH solution and then transfered to teflon autoclaves which was kept in an electric oven at 190 °C for 24 h. After cooling down to room temperature, the sample was washed with distilled water several times until the pH value of the washing solution was about 7.0 and then dried at 80 °C overnight in air. After being immersed in 0.1 mol/L HCl solution overnight, the sample was washed and dried again using the above method, and then TiO_2 nanowire precursor was obtained.

To prepare HTNWs precursor, the as-prepared TiO_2 nanowires precursor was immersed in $Ho(NO_3)_3$ aqueous solution at different concentrations of Ho_2O_3 overnight. After being filtered and washed with distilled water, different HTNWs precursors were obtained.

2.1.2 Synthesis of HTNWs

The HTNWs with different Ho_2O_3-doped contents were obtained by heating the corresponding precursor at 650 °C for 2 h in air. For the convenience of description, the HTNWs with Ho_2O_3-doped contents of 0, 2%, 4% and 6% (mass fraction) were labeled as S0, S1, S2 and S3, respectively.

2.2 Fabrication of DSSCs based on HTNWs photoanodes

The TiO_2 blocking layer for DSSCs was prepared according to the following strategy: tetrabutyl titanate was mixed with diethanolamine and absolute ethyl alcohol, and appropriate distilled water was added dropwise, then, the obtained colloidal sol was coated on FTO by spin-coating method, and the blocking layer film formed after being sintered at 500 °C for 30 min. In the next step, mesoporous HTNWs films were prepared through screen printing method as follows: firstly, appropriate HTNWs was added into the agate mortar in the presence of distilled water, acetic acid and triton X-100 to obtain the screen printing slurry. Secondly, the obtained slurry was screen printed on the blocking layer film and annealed at 500 °C for 30 min to remove the binders in the slurry. To prepare dye-sensitized electrodes, the mesoporous HTNWs film electrodes was immersed in 0.5 mmol/L N719 ethanol solution overnight at room temperature in the dark. After being removed from the dye solution, the electrodes were rinsed and dried. Finally, the unsealed sandwich type solar cells, assembled with dye sensitized HTNWs electrodes with Ho_2O_3 contents of 0, 2%, 4% and 6% (mass fraction) as the photoanodes, Pt coated FTO electrode as the counter electrode, and standard iodide electrolyte solution as a mediator, were labeled as W_0, W_1, W_2 and W_3, respectively. The area of working electrode was 0.25 cm^2.

2.3 Characterization

X-ray diffraction (XRD) experiments were carried out at room temperature using a D/max 3B diffractometer operated at 30 kV and 100 mA with Cu K_α radiation (λ=0.154 nm) to identify the crystal phase of samples. The surface morphology was examined using a scanning electron microscope (SEM, JSM−6460LV). Absorbance spectroscopy of samples was tested in an ultraviolet−visible absorbance spectrometer (UV−Vis, Lambda35). The photoluminescence (PL) spectra were analyzed using a fluorescence spectrometer (LS−55). A solar simulator (SS50) providing an illumination of AM1.5G simulated sunlight with 100 mW/cm^2 irradiation and a Keithley 2400 source meter were employed to measure the photovoltaic properties of the assembled DSSCs. The monochromatic incident photon−electron conversion efficiency (IPCE) of the DSSCs was also measured using a light meter (SM−25, Japan).

3 Results and discussion

3.1 Phase analysis

The XRD pattern of S2 with 4% Ho_2O_3 is shown in

Fig. 1. The peaks at 2θ values of 25.26°, 36.88°, 47.78°, 62.74° and 68.99° correspond to the (101), (004), (200), (204) and (116) crystal planes of anatase TiO_2, respectively. All the peaks can be perfectly indexed as a pure anatase phase of TiO_2 (JCPDS card No. 21−1272) with lattice constants a=3.7852 Å and c=9.5139 Å. Moreover, no other peaks are detected, which indicates that the crystal structure of TiO_2 is not changed by doping with a small amount of Ho^{3+} ions. Furthermore, in the case of raw TiO_2 samples, the transition of anatase to rutile phase started at around 600 °C, and the two phases co-existed in a wide temperature range (from 600 to 900 °C) [20,21]. While, all peaks of the as-prepared samples can be assigned to the anatase phase calcined at 650 °C. As suggested by other authors, the rare earth element dopant influences the transition rates of anatase to rutile TiO_2 phase due to perturbation in the crystal nucleation process for either substitutional or interstitial dopant ion incorporation within the host lattice [22,23]. Indeed, the rare earth ion incorporation within the titania structural framework causes lattice site distortions due to the large difference of ionic radii between Ti^{4+}(0.68 Å) and Ho^{3+} (90.1 Å).

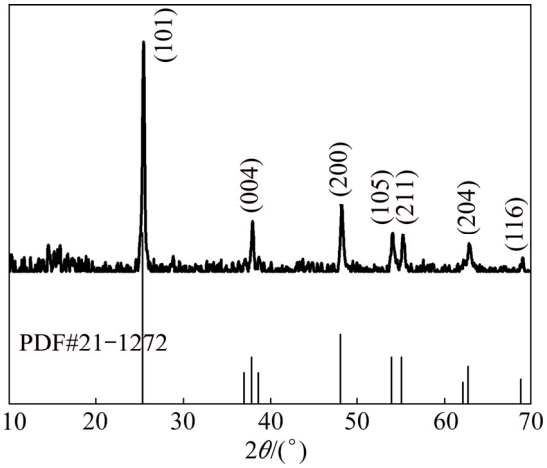

Fig. 1 XRD pattern of S2 with 4% Ho_2O_3

3.2 Morphology analysis

Figures 2(a) and (b) show the SEM images of S0 and S2, respectively. As shown in Fig. 2(a), after hydrothermal reaction for 24 h, the high purity TNWs with large aspect ratio are obtained. After hydrothermal reaction, P25 nanoparticles were transformed into non-hollow nanowires with small size distributions both in length and in diameter. Approximately, the lengths are 2−20 μm and the diameters are 100−200 nm. Figure 2(b) shows the SEM image of the HTNWs with 4% Ho_2O_3 (S2). Compared with the pure TNWs, the HTNWs keep the original appearance and display highly porous network morphology. The magnified image shows that the network consists of ultrafine HTNWs with an average diameter of 150 nm.

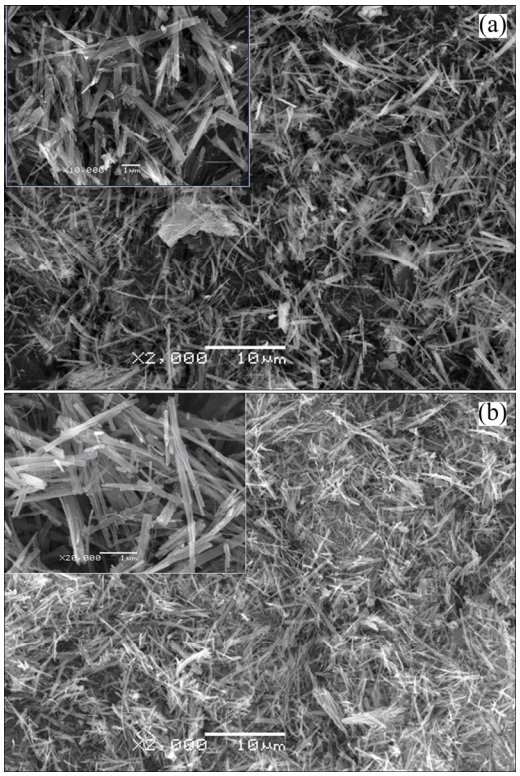

Fig. 2 SEM images of S0 (a) and S2 (b)

3.3 Downconversion (DC) luminescence analysis

The excitation (emission at 587 nm) and emission spectra (excited at 412 nm) of S1−S3 with Ho_2O_3 of 2%, 4% and 6% in sequence are shown in Fig. 3. It can be seen that HTNWs possess an obvious luminescence function. A significant excitation peak at 412 nm and an emission peak at 587 nm are observed. The excitation peak at 412 nm and the emission peak at 587 nm corresponded to the Ho^{3+}:$^5I_8 \rightarrow {}^5G_5$, $^5S_2 \rightarrow {}^5I_8$ transitions, respectively. The luminescence at 587 nm is just within the absorption wavelength range of sensitizing dye N719. Combining the excitation and emission spectra, the ultraviolet irradiation can be absorbed by the N719 dye in the DSSCs via the conversion luminescence of HTNWs and the solar light harvest of DSSCs may thus increase. Figure 4 shows the PL intensity of HTNWs as a function of doping content of Ho_2O_3. According to the emission spectra, the relative PL intensity of HTNWs decreases slightly with the increase of Ho_2O_3 content from 2% to 4%. But larger amount of Ho_2O_3 (6%) because of filling the quenching sites decreases the PL intensity obviously. Figure 5 shows the energy-level diagram of Ho^{3+} and DC mechanisms. According to the energy band and energy matching between the excitation and emission wavelength, the possible DC energy transfer mechanism is suggested that ultraviolet photon excitation (at 412 nm) makes the electron of Ho^{3+} excited

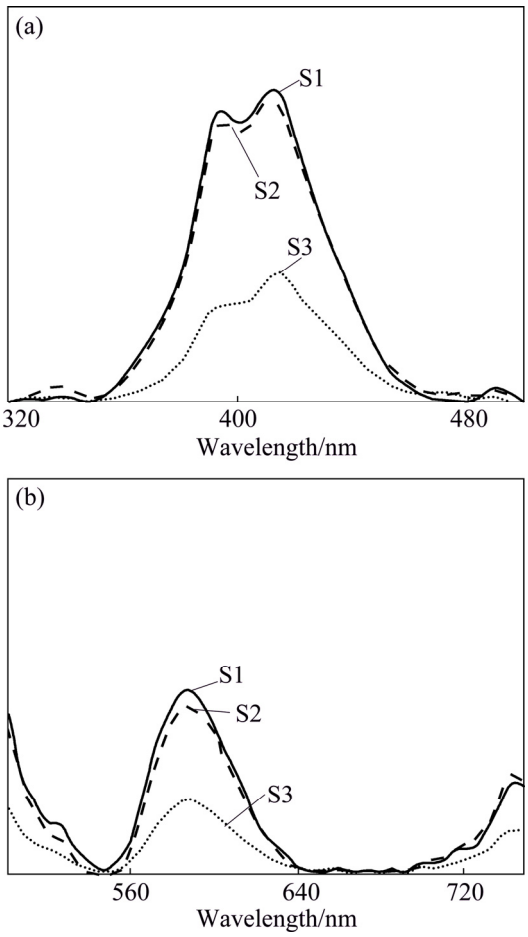

Fig. 3 Excitation (a) and emission (b) spectra of S1−S3 with Ho_2O_3 of 2%, 4% and 6% in sequence

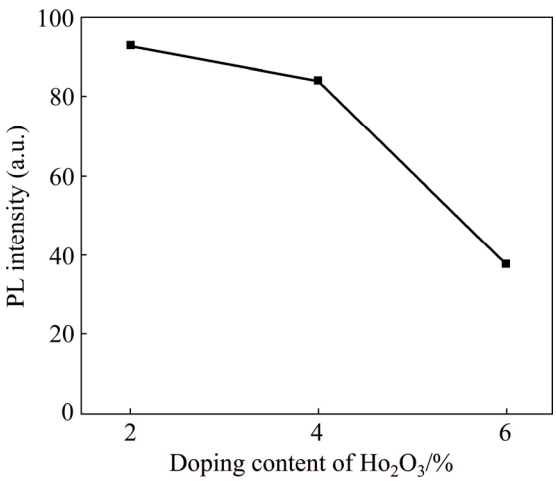

Fig. 4 PL intensity of HTNWs as function of doping content of Ho_2O_3 at 587 nm

to a higher energy state ($^5G_5$), where radiationless transition occurs until the electron resides at the $^5S_2$ energy level in 4f shell. Then, radiative transition occurs to the $^5I_8$ ground state ($^5S_2 \rightarrow {}^5I_8$) and generates green light emission around 587 nm.

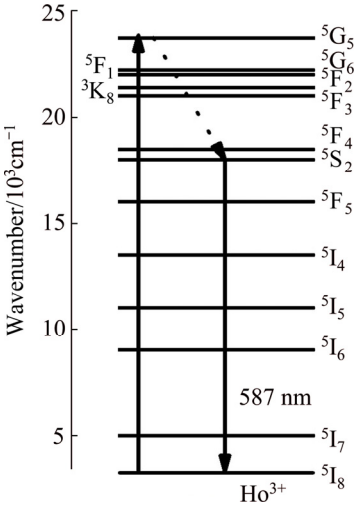

Fig. 5 Schematic energy level diagram of Ho^{3+} in TiO_2 and DC mechanisms on excitation by 412 nm radiation (Full and dotted arrows indicate radiative emission and energy transfer, respectively)

3.4 Analysis of UV−Vis absorption spectra

The optical properties of TNWs with different Ho^{3+}-doped contents in the range of 300−700 nm were studied by the UV−Vis absorption spectra and the results are shown in Fig. 6. All the samples have absorbance in the UV−Vis region. In addition, in the wavelength around 330 nm, the photoanodes with HTNWs (S2, S3) show more absorption. The possible reason is that the HTNWs could absorb and convert near and middle ultraviolet light to visible light which the N719 could absorb easily. Furthermore, the photoanodes with strong absorbance effects would improve the light-harvesting efficiency resulting in a higher current density, and the highest absorption spectrum in the case of HTNWs doped with 4% Ho_2O_3 is consistent with its highest short-circuit current density (J_{sc}) of the relevant DSSCs. In all, the highest efficiency of 1.03% is obtained for the DSSCs with HTNWs doped with 4% Ho_2O_3.

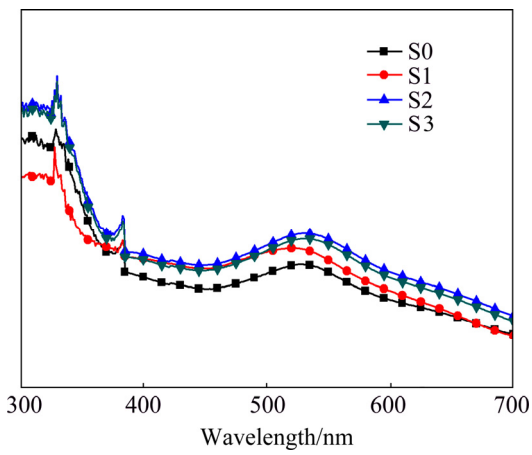

Fig. 6 UV−Vis absorbance spectra of different photoanodes sensitized with N719

3.5 Photoelectric properties of DSSCs

Figure 7 shows the current density−voltage curves of W0−W3 DSSCs based on the films of DC HTNWs with different doping contents of Ho_2O_3. The open circuit voltage (φ), short-circuit current density (J_{sc}), fill factor (F_f) and photoelectric conversion efficiency (η) of these DSSCs are summarized in Table 1, while Fig. 8 shows the dependence of J_{sc} and η on the Ho_2O_3 doping content in TNWs. As shown in Fig. 8, the photocurrent density and conversion efficiency first increase and then decrease with increasing the doping content of Ho_2O_3, and the open circuit voltage is similar. When the doping content of Ho_2O_3 reaches 4%, the photocurrent density and the conversion efficiency of the cell peak reach the optimum values of 5.6 mA/cm^2 and 1.93%, respectively. As the doping content increases beyond 4%, both the photocurrent density and conversion efficiency decrease. The increase of J_{sc} when the doping amount is less than 4% can be attributed to the DC luminescence of Ho^{3+} from ultraviolet light to visible light. Moreover, the changes of TiO_2 energy level by doping rare-earth ions improve the carrier transport at the interface of TiO_2/Dye, which further improves the J_{sc}. However, when the amount of Ho_2O_3 is beyond 4%, more grains, phases and domain interfaces are produced in the doping layer. These interfaces can capture photo-generated electrons and holes, hindering the charge carrier transportation, leading to a decrease of photocurrent [24]. This is the reason why J_{sc} increases first and then decreases with the increase of Ho_2O_3 content in the TiO_2 layer of the DSSCs.

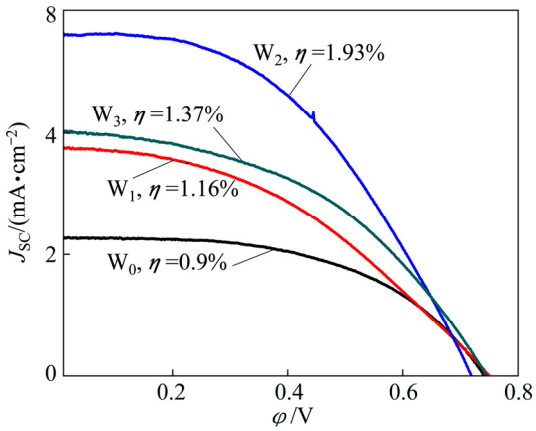

Fig. 7 J_{sc}−φ curves of W0−W3 DSSCs

Table 1 Property parameters of W0−W3 DSSCs

Cell	φ/V	J_{sc}/(mA·cm^{-2})	F_f	η/%
W0	0.74	2.27	0.53	0.9
W1	0.75	3.74	0.41	1.16
W2	0.72	5.6	0.48	1.93
W3	0.75	4.04	0.45	1.37

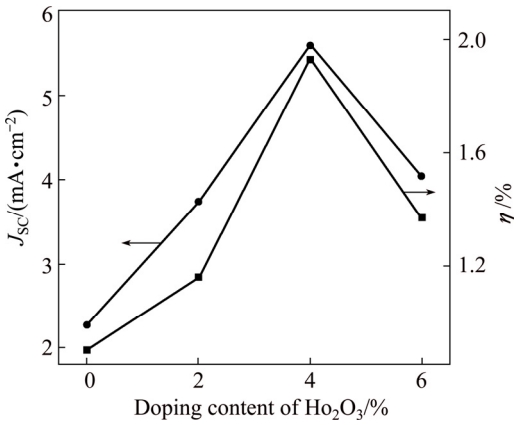

Fig. 8 Dependence of J_{sc} and η on doping content of Ho_2O_3

In addition, the J_{sc} is also reflected in the IPCE performance (Fig. 9). The cell with 4% Ho_2O_3 shows the maximum IPCE of 33.25% at 520 nm, while the IPCE value of the cell without Ho_2O_3 is only 7.8%. This indicates that the significant improvement of J_{sc} is due to the enhancement of the photo-to-current efficiency.

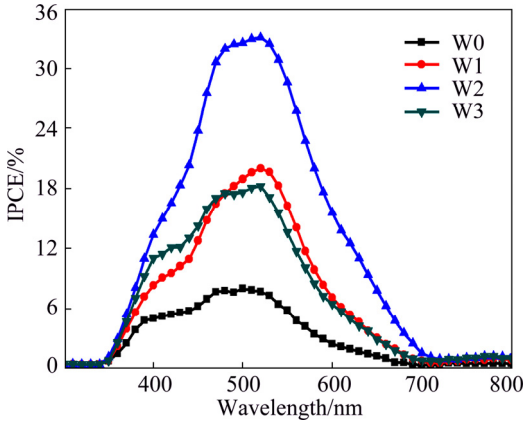

Fig. 9 IPCE curves of W0−W3 DSSCs

4 Conclusions

1) As a conversion luminescence medium, the HTNWs broaden the near and middle ultraviolet light harvest via DC luminescence and increase the photocurrent.

2) When the doping content of Ho_2O_3 is 4%, the photoelectric conversion efficiency of the DSSC is two-fold increase compared with that of the DSSC without Ho^{3+} ions.

3) The research results reveal that the DC material HTNW is helpful to improve the performance of DSSCs.

References

[1] KUMAR A, KANDPAL T C. Renewable energy technologies for irrigation water pumping in India: A preliminary attempt towards potential estimation [J]. Energy, 2007, 32: 861−870.

[2] HSIAO Y C, WU T F, WANG Y S, HU C C, HUANG C. Evaluating the sensitizing effect on the photocatalytic decoloration of dyes using

anatase-TiO_2[J]. Appl Catal B−Environ, 2014, 148: 250−257.

[3] NIU Hai-jun, MU Jing-shan, ZHANG Mi-lin, LUO Jun, LUO Pei-hui, BAI Xu-duo, WANG Wen. Naphthalene-containing polyimides: Synthesis, characterization and photovoltaic properties of novel donor-acceptor dyes used in solar cell [J]. Transactions of Nonferrous Metals Society of China, 2009, 19(S3): s587−s593.

[4] SINGH H K, AGARWAL D C, CHAVHAN P M, METRA R M, AGGARWAL S, KULRIYA P K, TRIPATHI A, AVASTHI D K. Study of swift heavy ion irradiation effect on indium tin oxide coated electrode for the dye-sensitized solar cell application[J]. Nucl Instrum Meth B, 2010, 268: 3223−3226.

[5] BASTIANINI M, VIVANI R, NOCCHETTI M, COSTENARO D, BISIO C, OSWALD F, MEYER T B, MARCHESE L. Effects of iodine intercalation in nanosized layered double hydroxides for the preparation of quasi-solid electrolyte in DSSC devices[J]. Sol Energy, 2014, 107: 692−699.

[6] LAI Hong-mei, WANG Yuan-zhe, DU Guo-ping, LI Wang, HAN Wei-zhi. Dual functional $YVO_4:Eu^{3+},Bi^{3+}@SiO_2$ submicron-sized core-shell particles for dye-sensitized solar cells: Light scattering and down-conversion [J]. Ceram Inter, 2014, 40: 6103−6108.

[7] EI-NAHASS M M, ALI M H, EI-DENGLAWEY A. Structural and optical properties of nano-spin coated sol-gel porous TiO_2 films[J]. Transactions of Nonferrous Metals Society of China, 2012, 22: 3003−3011.

[8] JANG H, YUN J, KIM D, NA S I, KIM S S. Transparent graphene oxide–Pt composite counter electrode fabricated by pulse current electrodeposition for dye-sensitized solar cells [J]. Surf Coat Tech, 2014, 242: 8−13.

[9] GRATZEL M. Solar energy conversion by dye-sensitized photovoltaic cells [J]. Inorg Chem, 2005, 44: 6841−6851.

[10] LAW M, GREENE L, JOHNSON J, SAYKALLY R, YANG P. Nanowire dye-sensitized solar cells [J]. Nat Mater, 2005, 4: 455−459.

[11] MOTLAK M, AKHTAR M, BARAKAT N. High-efficiency electrode based on nitrogen-doped TiO_2 nanofibers for dye-sensitized solar cells [J]. Electrochim Acta, 2014, 115: 493−498.

[12] SHALAN A E, RASHAD M M, YU Y H, LIRA-CANTU M, ABDEL-MOTTALEB M S A. Controlling the microstructure and properties of titania nanopowders for high efficiency dye sensitized solar cells [J]. Electrochim Acta, 2013, 89: 469−478.

[13] ONO T, YAMAGUCHI T, ARAKAWA H. Study on dye-sensitized solar cell using novel infrared dye [J]. Sol Energy Mater Sol Cells, 2009, 93: 831−835.

[14] LI Qing-bei, LIN Jian-ming, WU Ji-huai, LAN Zhang, WANG Yue, PENG Fu-guo, HUANG Miao-liang. Improving photovoltaic performance of dye-sensitized solar cell by downshift luminescence and p-doping effect of $Gd_2O_3:Sm^{3+}$ [J]. J Lumin, 2013, 134: 59−62.

[15] LI Liang, YANG Yu-lin, ZHOU Mi, FAN Rui-qing, QIU Le-le, WANG Xin, ZHANG Ling-yun, ZHOU Xue-song, HE Jiang-long. Enhanced performance of dye-sensitized solar cells based on TiO_2 with NIR-absorption and visible up-conversion luminescence [J]. J Solid State Chem, 2013, 198: 459−465.

[16] SENTHIL T S，KIM D J, MUTHUKUMARASAMY N, KANG M. Closely packed dense network rutile nanorods with gadolinium for efficient dye sensitized solar cells [J]. Appl Surf Sci, 2014, 313: 858−863.

[17] CAO Yue-chan, ZHAO Zong-yan, YI Juan, MA Chen-shuo, ZHOU Da-cheng, WANG Rong-fei, LI Chen, QIU Jian-bei. Luminescence properties of Sm^{3+}-doped TiO_2 nanoparticles: Synthesis, characterization, and mechanism [J]. J Alloy Compd, 2013, 554: 12−20.

[18] RESZCZYNSKA J, GRZYB T, SOBCZAK J, LISOWSKI W, GAZDA M, OHTANI B, ZALESKA A. Lanthanide co-doped TiO_2: The effect of metal type and amount on surface properties and photocatalytic activity [J]. Appl Surf Sci, 2014, 307: 333−345.

[19] LI Yue-ying, HAO Hong-shun, QIN Lei, WANG Hui-li, NIE Ming-qi, HU Zhi-qiang, GAO Wen-yuan, LIU Gui-shan. Synthesis and characterization of Ho^{3+}-doped strontium titanate downconversion nanocrystals and its application in dye-sensitized solar cells [J]. J Alloy Compd, 2015, 622: 1−7.

[20] VERISSIMO N C, CREMASCO A, RODRIGUES C A, BERTAZZOLI R, CARAM R. In situ characrerization of the effects of Nb and Sn on the anntase-rutile transition in TiO_2 nanotubes using high-temperature X-ray diffraction [J]. Appl Surf Sci, 2014, 307: 372−381.

[21] CHEN Qing-hua, LIU Hui-ling, XIN Yan-jun, CHENG Xiu-wen. TiO_2 nanobelts–Effect of calcination temperature on optical photoelectrochemical and photocatalytic properties [J]. Electrochim Acta, 2013, 111: 284−291.

[22] VRANJES M, KULJANIN-JAKOVLJEVIC J, AHRENKIEL S P, ZEKOVIC I, MITRIC M, SAPONJIC Z, NEDELJKOVIC J M. Sm^{3+} doped TiO_2 nanoparticles synthesized from nanotubular precursors-luminescent and structural properties [J]. J Lumin, 2013, 143: 453−458.

[23] KRALCHEVSKA R, MILANOVA M, HRISTOV D, PINTAR A, TODOROVSKY D. Synthesis, characterization and photocatalytic activity of neodymium, nitrogen and neodymium–nitrogen doped TiO_2 [J]. Mater Res Bull, 2012, 47: 2165−2177.

[24] KO K H, LEE Y C, JUNG Y J. Enhanced efficiency of dye-sensitized TiO_2 solar cells (DSSC) by doping of metal ions [J]. J Colloid Interf Sci, 2005, 283: 482−487.

$TiO_2:Ho^{3+}$纳米线下转换光阳极的制备及其光电性能

李月英[1,2,3]，郝洪顺[1,2,3]，王丽君[1,2,3]，郭伟华[1,2,3]，苏 青[1,2,3]，
秦 磊[3]，高文元[1,2,3]，刘贵山[1,2,3]，胡志强[1,2,3]

1. 大连工业大学 无机非金属材料工程系，大连 116034；
2. 大连工业大学 新材料与材料改性省高校重点实验室，大连 116034；
3. 大连工业大学 国家海洋食品工程技术研究中心，大连 116034

摘 要：采用水热法制备 TiO_2 纳米线前驱体，将其浸入 $Ho(NO_3)_3$ 水溶液并取出煅烧，得到 $TiO_2:Ho^{3+}$下转换纳米线，用其制备染料敏化太阳能电池的光阳极，探讨其光电性能。用扫描电镜和 X 射线衍射分别表征 $TiO_2:Ho^{3+}$纳米线的形貌和结构。荧光光谱和紫外−可见吸收光谱显示 $TiO_2:Ho^{3+}$下转换纳米线可以将近紫外光和中紫外光转化为可以被 N719 染料吸收的可见光。与纯 TiO_2 纳米线作为光阳极的电池相比，以 $TiO_2:Ho^{3+}$下转换纳米线作为光阳极的电池有较好的光电转换效率，且当 Ho^{3+}掺杂量为 4%时(质量分数)，电池效率提高了一倍。$TiO_2:Ho^{3+}$下转换纳米线拓宽光谱响应范围至近紫外光和中紫外光区，提高了电池的短路电流密度，从而电池效率提高。

关键词：$TiO_2:Ho^{3+}$纳米线；下转换荧光；染料敏化太阳能电池；光伏性能

(Edited by Mu-lan QIN)